Internal Structure of the Jets in 3C 353

Mark R. Swain[1] and Alan H. Bridle
National Radio Astronomy Observatory[2],
520 Edgemont Road, Charlottesville, VA 22903-2475

and

Stefi A. Baum
Space Telescope Science Institute,
2700 San Martin Drive, Baltimore, MD 21218

ABSTRACT

We have imaged the total and polarized intensity structures of the jets in the FR II radio galaxy 3C 353 with transverse resolutions up to nine beamwidths using the VLA at 8.4 GHz. Both the polarized intensity and the apparent degree of linear polarization exhibit elongated *minima* near both edges of both jets. We interpret these minima as the result of vector cancellation along the line of sight between polarized emission from the outer layers of the jets and from the surrounding lobes. Both jets also exhibit flat-topped total intensity profiles over much of their length.

We infer that most of the jet emission comes from a thick outer layer where the magnetic field has no component transverse to the jet axis, but the axial and toroidal components are random and approximately in equipartition. We suggest that this region is a boundary layer where the field is ordered by velocity shear. The *apparently* lower emissivity near the jet axis may be produced by Doppler hiding of emission from fast-flowing material in the jet "spines". This view of the internal structure of an FR II jet can readily be unified with the two-component model for decelerating FR I jets proposed by Laing (1993, 1996).

Subject headings: galaxies:jets — radio continuum: galaxies — magnetic fields — polarization

1. Introduction

3C 353 is the fourth strongest radio galaxy in the 3C Catalogue (flux density 57 Jy at 1.4 GHz). The host is a V=15.4-magn elliptical galaxy at z=0.0304, the dominant member of a Zwicky cluster. 3C 353's projected linear size is $120h^{-1}$ kpc, and its monochromatic luminosity $P_{1.4\,\mathrm{GHz}}$ is $\sim 5h^{-2} \times 10^{25}$ W Hz^{-1} for $H_0 = 100h$ km s^{-1} Mpc^{-1}. The source contains a well-collimated jet and counterjet (Swain, Bridle, & Baum 1996), differing by a factor of ~ 2 in integrated flux density, and together comprising $\lesssim 1\%$ of the total emission. The lobe morphology, the clear hot spot in the jetted lobe, and the source's position in the

---

[1]now at: Astronomy Department, Cornell University, Ithaca, NY 14850

[2]The NRAO is a facility of the National Science Foundation, operated under co-operative agreement by Associated Universities, Inc.

bivariate optical-radio luminosity domain (Owen & Ledlow 1994), are all consistent with classifying 3C 353 as an FR Type II source (Fanaroff & Riley 1974).

We report VLA 8.4-GHz imaging of the total and polarized emission of 3C 353 that shows the internal structure of kpc-scale jets in this FR II source at unusually high spatial resolution (FWHM $185h^{-1}$ pc in projection). We also present a simple model for this structure.

2. The Observations

The 8.4 GHz observations were made with two pointings of the VLA in each of its A, B, C and D configurations. The data from all four configurations were combined, self-calibrated and deconvolved as described by Swain (1996). The final images were restored with circular Gaussian beams of FWHM $0\farcs44$, and have rms noise of 19 μJy per CLEAN beam area in Stokes I and 16 μJy per CLEAN beam area in Stokes Q and U. Figure 1 (Plate L1) shows the I image as a gray scale, with salient features labeled. Both jets are first detected $\sim 10h^{-1}$ kpc from the nucleus. The brighter jet can be traced continuously from J1 until it enters a well-defined hot spot (H). The counterjet is detected unambiguously only at CJ1 and CJ2; it is unclear where it terminates.

3. The Jet and Counterjet

The transverse widths Φ of both jets grow only slowly, if at all, with increasing distance Θ from the nucleus, after they first brighten. Their full opening angles, $\arctan(d\Phi/d\Theta)$, are $0\fdg85 \pm 0\fdg26$ (jet) and $1\fdg12 \pm 0\fdg27$ (counterjet). These estimates are the averages of the regression slopes against Θ of five different measures of Φ: FWHM, 3σ and 5σ isophote separation, equivalent rectangular width, and the separation of the steepest transverse brightness gradients (Swain 1996).

Neither jet is prominent in polarized *emission* $P = \sqrt{Q^2 + U^2}$, but there are distinct, linear *minima* in P near both edges of both jets, giving an appearance of parallel dark "rails" in the P images. Figure 2 shows how these rails are related to total intensity (I) profiles taken transverse to the jets. Because neither jet nor the rail separation expands significantly between the bright knots J1 and J4, the jet profiles are *averaged* over this region. The counterjet profiles are averaged over the short feature CJ2. The "noise" is less in the jet average because the averaging region is fourteen times longer than for the counterjet.

Note the following features of Figure 2:

1. The mean profiles of both jets in total intensity are well-resolved and essentially flat-topped.
2. The polarization minima, or "rails", occur close to the steepest transverse intensity gradients of the jets.
3. There is little excess (i.e. jet-related) polarized emission between these rails. The apparent degree of linear polarization of the jet emission near the jet axis is typically $< 10\%$, and reaches 20% only at the penultimate jet knot, J4.

We also imaged 3C 353 using the VLA at 1.4, 1.7 and 4.9 GHz at $1\farcs3$ resolution (Swain 1996). These images showed that the location and shape of the polarization rails, and their depth (as a fraction of the jet emission in their vicinity) change little between 1.4 and 8.4 GHz.

4. Origin of the Polarization "Rails"

In principle, there are three ways that such elongated polarization minima could be formed:

1. They could mark elongated regions of intrinsically low polarization in both lobes that are aligned beside (essentially) unpolarized jets.
2. They could result from depolarization of the lobe and jet emission by an inhomogeneous Faraday screen localized near the jets.
3. They could arise by vector cancellation of orthogonally polarized emission components along the line of sight, if the jets and the lobes contain distinctly different magnetic field configurations.

The first interpretation is unlikely because the decrease in polarized intensity P at the rails is often 30% to 50% of the *polarized* emission from the lobe on adjacent sightlines. Improbable geometries (slab-like features in the lobes with their long axes aligned with the line of sight) would therefore be needed to generate low-polarization regions on both sides of the jets. The second interpretation is highly unlikely because the fractional depth and separation of the rails changes little between 1.4 and 8.4 GHz, and because our four-frequency data reveal no unusual Faraday rotation features near the jet (Swain 1996).

The third interpretation, vector cancellation, is compatible with all of our data. The *apparent* magnetic field direction $\mathbf{B_a}$ inferred in the lobes, after correction for Faraday rotation, is approximately *perpendicular* to the jet axis along most of the length of both jets. If sightlines through the outer layers of these jets, but not those through their centers, are dominated by $\mathbf{B_a}$ *parallel* to the jet axes, then the net polarized intensity can have minima near the jet edges, as observed.

Figure 3 shows that the "rail depth" (the difference between the local minimum in P and the value interpolated from the ambient polarized emission), correlates well with the total intensity I of the jet at the position of the minimum, everywhere the rail depth exceeds 3σ. (The jet total intensity was determined by fitting and removing the lobe background from each profile using a low-order polynomial). The only badly discrepant point comes from the south edge of knot J1, where a rail is detected but the intensity profiles differ significantly from the mean. We infer that:

1. The rails are a feature of the jet, not of the lobe, emission. The rails are also not seen anywhere that the jet is not detected.
2. The average degree of linear polarization (P/I) of the jet component that is responsible for the rails in the vector-cancellation model must be $\sim$ 20 to 30%, similar to that found directly in the polarized *emission* of other FR II jets (e.g. Bridle & Perley 1984, Bridle et al. 1994).
3. In the vector-cancellation model, the polarization structure of the jet and of the background must both be roughly constant along the jet, as strong variations in either would corrupt this correlation.

The rail minima never go to zero, so the polarized jet emission never completely cancels that from the rest of the line of sight. In the few places where the polarized intensity between the rails is *positive* with respect to the ambient polarization, the apparent magnetic field near the jet axis must therefore be *perpendicular* that axis, to reinforce the lobe polarization.

We now present a simple model for the jet that is consistent with these results.

5. Modeling

The correlation shown in Figure 3, the slow (zero) spreading rate of the jet, and the constant separation of the "rails" are consistent with a jet whose structure is approximately self-similar everywhere between J1 and J4. We therefore modeled the *averaged* transverse I and P profiles, rather than individual profiles, to improve our signal-to-noise.

We use r, ϕ, z coordinates in a cylindrical jet axisymmetric about the z axis and inclined by angle i to the plane of the sky. The jet is populated by relativistic electrons with a power-law energy distribution, a specified emissivity distribution, and a specified magnetic field geometry, including both organized and random components. The transverse I, Q and U profiles are computed by integrating 1301 equal cells along each of 131 equally-spaced lines of sight through the jet, and are then convolved to the resolution of our data. We matched the index of the power-law electron energy distribution to the flattest spectral index associated with the jets ($\alpha = -0.65$); our results are insensitive to this choice.

Figure 4 shows the average transverse I and P profiles that we infer by assuming that the lobe magnetic field is perpendicular to both jets everywhere. These profiles are fitted well by a model (also shown) in which

1. the jets are in the plane of the sky ($i = 0°$),
2. the radiating particles are restricted to an outer layer ($r \geq r_{\rm min} \sim 0.43$ of the radius of the jet),
3. this outer layer has no radial field component B_r,
4. B_ϕ (toroidal) and B_z (axial) in the layer are uniformly distributed zero-mean random variables normalized so that $\langle B_\phi^2 \rangle^{1/2} = \langle B_z^2 \rangle^{1/2}$.

The value of $r_{\rm min}$ in this model is a compromise between the optimal fits for the jet and the counterjet. For the jet, the ranges of parameters that fit the observed I and P profiles within their 2σ errors everywhere, holding the other parameters fixed, are $0.48 \leq r_{\rm min} \leq 0.53$, $0.9 \leq \langle B_\phi^2 \rangle^{1/2} / \langle B_z^2 \rangle^{1/2} \leq 1.1$, and $0° \leq i \leq 30°$. The best-fitting values of $r_{\rm min}$ in the counterjet are $\sim 20\%$ smaller.

Such models with *no* emission from the jet "spine" at $r < r_{\rm min}$ predict the observed I profiles to within their errors, but in detail the model profiles are too edge-brightened. Better fits are obtained if the spine also radiates, but with an emissivity less than half that of the outer layer, and if the spine field has $B_z = 0$.

The constraints imposed by fitting the I and P profiles simultaneously are strong, so it is unlikely that any fundamentally dissimilar models of magnetic field organization and relative emissivity will fit our data so well. A smaller ratio of B_ϕ to B_z can however be traded against orienting the jet away from the plane of the sky to some extent: models with B_z as the *only* field component in the radiating layer can reproduce the observed flat-topped I profiles, but they over-predict the degree of linear polarization at the rail centers, typically by a factor of two. We also computed the emission from several well-ordered field structures previously proposed for large-scale jets, including helical fields and transverse self-similar "flux ropes" (Chan & Henriksen 1980). We found none that simultaneously produced flat-topped I profiles and symmetric P profiles with ~ 20 to 30% polarization (Swain 1996).

6. Discussion

The average I and P profiles of 3C 353's jets are modeled well by the emission from a thick, constant-depth, boundary layer containing a random magnetic field with no component B_r perpendicular to the jet flow. We associate this layer with a region where B_r is suppressed by velocity shear (presumably faster flow at the center of the jet and slower flow at its surface). The roughly constant layer depth and degree of linear polarization along the jet, plus the absence of B_r, imply that the radiating layer does not contain large-scale turbulent eddies associated with entrainment of ambient material (De Young 1996).

The model has a simple relation to the decelerating relativistic-jet model for the first few kpc of FR I (plumed) sources (Laing 1993, Laing 1996, Laing & Bridle, in preparation). The field configuration $(B_r = 0, B_\phi \sim B_z)$ in the outer layer is similar to that inferred by Laing & Bridle in the outer layer of the *rapidly*-spreading jets in the FR I radio galaxy 3C 31, but in 3C 353 the layer has constant depth and the jets spread slowly. The *apparently* low emissivity of 3C 353's jet spine could also be due to Doppler "hiding" of a faster (relativistic) flow near the jet axis.

If parts of 3C 353's jets move relativistically, we have modeled their appearance *in our rest frame.* Relativistic aberration modifies the angle of the fields to the line of sight, so our best fit may correspond to to a different ratio of $\langle B_\phi^2 \rangle^{1/2}$ to $\langle B_z^2 \rangle^{1/2}$ in the jet's frame, depending on the velocity field in the outer layer. The modification will be within our uncertainties if the velocities in the outer layer are not too high. For example, the parameter ranges that fit our data to within their 2σ errors imply that we could fit the observed profiles with a jet at 15° to the sky, $v < 0.5c$ and $B_\phi \sim B_z$ everywhere in the outer layer, and $v > 0.8c$ in the spine (to produce the Doppler hiding of this region). The spine field geometry is poorly constrained by our data, except that it cannot be dominated by B_z. If $v \sim 0.5c$ everywhere in the outer layer, then Doppler favoritism would also produce a 2:1 jet-counterjet intensity asymmetry. As the observed counterjet in 3C 353 is not just a faint replica of the main jet, some intrinsic asymmetry must also be present. Parts, or all, of the outer-layer flow may therefore have $v < 0.5c$. A relativistic-jet scenario in which the fields in the jet's frame might differ substantially from our model is that of a high-velocity $(v \gtrsim 0.8c)$ outer-layer flow close enough to the plane of the sky that Doppler *favoritism* is small (to keep a $\lesssim$ 2:1 intensity ratio between the jets) but in which the *aberration* is large.

7. Conclusions

The polarization "rails" at the edges of 3C 353's jets result from vector cancellation between polarized jet emission and orthogonally polarized lobe emission. The flat-topped I profiles and the *apparently* parallel $(B_r \rightarrow 0)$ magnetic field in the outer layers of 3C 353's jets resemble features of other well-resolved FR II jets (Cygnus A: Carilli et al. 1996; 3C 219: Bridle, Perley, & Henriksen 1984, Perley, Bridle, & Clarke 1994). We therefore support the suggestion (Bridle & Perley 1984) that much of the emission from FR II jets originates in a thick shear layer. The emissivity distribution deduced for 3C 353 could be explained by *in situ* particle acceleration in the shear layer (as proposed for M 87 by Owen, Hardee, & Cornwell 1989) or by Doppler hiding of emission from the jet "spine". Doppler hiding would fit the following view of relationships between FR I and FR II jets:

1. All AGN radio jets initially contain a relativistically-moving spine surrounded by a slower-moving shear layer (Laing 1993, Laing 1996).
2. The shear layer contains B_ϕ and B_z roughly in equipartition, but little B_r; the spine contains little

B_z.

3. The spine decelerates to sub-relativistic speeds a few kpc from the nucleus in FR I sources, but not in FR II sources (Bicknell 1995).

4. In FR II sources, the observed "jet" emission comes mostly from the shear layer, but in FR I sources the spine emission becomes visible where the spine decelerates, a few kpc from the AGN.

If this view is correct, then similarly well-resolved radio jets in FR II *quasars* will be more strongly center-brightened, and their counterjets more strongly limb-brightened, than those in FR II radio galaxies, because the Doppler asymmetries are greater in jets that are closer to the line of sight.

We thank Robert Laing and the referee for helpful advice and comments.

REFERENCES

Bicknell, G. V. 1995, ApJS, 101, 29

Bridle, A. H., & Perley, R. A. 1984, ARA&A, 22, 319

Bridle, A. H., Hough, D. H., Lonsdale, C. J., Burns, J. O., & Laing, R. A. 1994, AJ, 108, 766

Bridle, A. H., Perley, R. A., & Henriksen, R. N. 1984, AJ, 92, 534

Carilli, C. L., Perley, R. A., Bartel, N., & Dreher, J. W. 1996, in Cygnus A - Study of a Radio Galaxy, ed. C. L. Carilli & D. E. Harris, (Cambridge: CUP), 76

Chan, K. L., & Henriksen, R. N. 1980, ApJ, 241, 534

De Young, D. S. 1996, in ASP Conference Series, Vol. 100, Energy Transport in Radio Galaxies and Quasars, ed. P. E. Hardee, A. H. Bridle, & J. A. Zensus (San Francisco: ASP), 261

Fanaroff, B. L., & Riley, J. M. 1974, MNRAS, 167, 31

Laing, R. A. 1993, in Space Telescope Science Institute Symposium 6, Astrophysical Jets, ed. D. Burgarella, M. Livio, & C. O'Dea (Cambridge: Cambridge University Press), 95

Laing, R. A. 1996, in ASP Conference Series, Vol. 100, Energy Transport in Radio Galaxies and Quasars, ed. P. E. Hardee, A. H. Bridle, & J. A. Zensus (San Francisco: ASP), 241

Owen, F. N., Hardee, P. E., & Cornwell, T. J. 1989, ApJ, 362, 449

Owen, F. N., & Ledlow, M. J. 1994, in ASP Conference Series, Vol. 54, The Physics of Active Galaxies, ed. G. V. Bicknell, M. A. Dopita, & P. J. Quinn (San Francisco: ASP), 319

Perley, R. A., Bridle, A. H., & Clarke, D. A. 1994, in Sub-arcsecond Radio Astronomy, ed. R. J. Davis & R. S. Booth (Cambridge: Cambridge University Press), 258

Swain, M. R. 1996, Ph.D. Thesis, U. Rochester

Swain, M. R., Bridle, A. H., & Baum, S. A. 1996, in ASP Conference Series, Vol. 100, Energy Transport in Radio Galaxies and Quasars, ed. P. E. Hardee, A. H. Bridle, & J. A. Zensus (San Francisco, ASP), 299

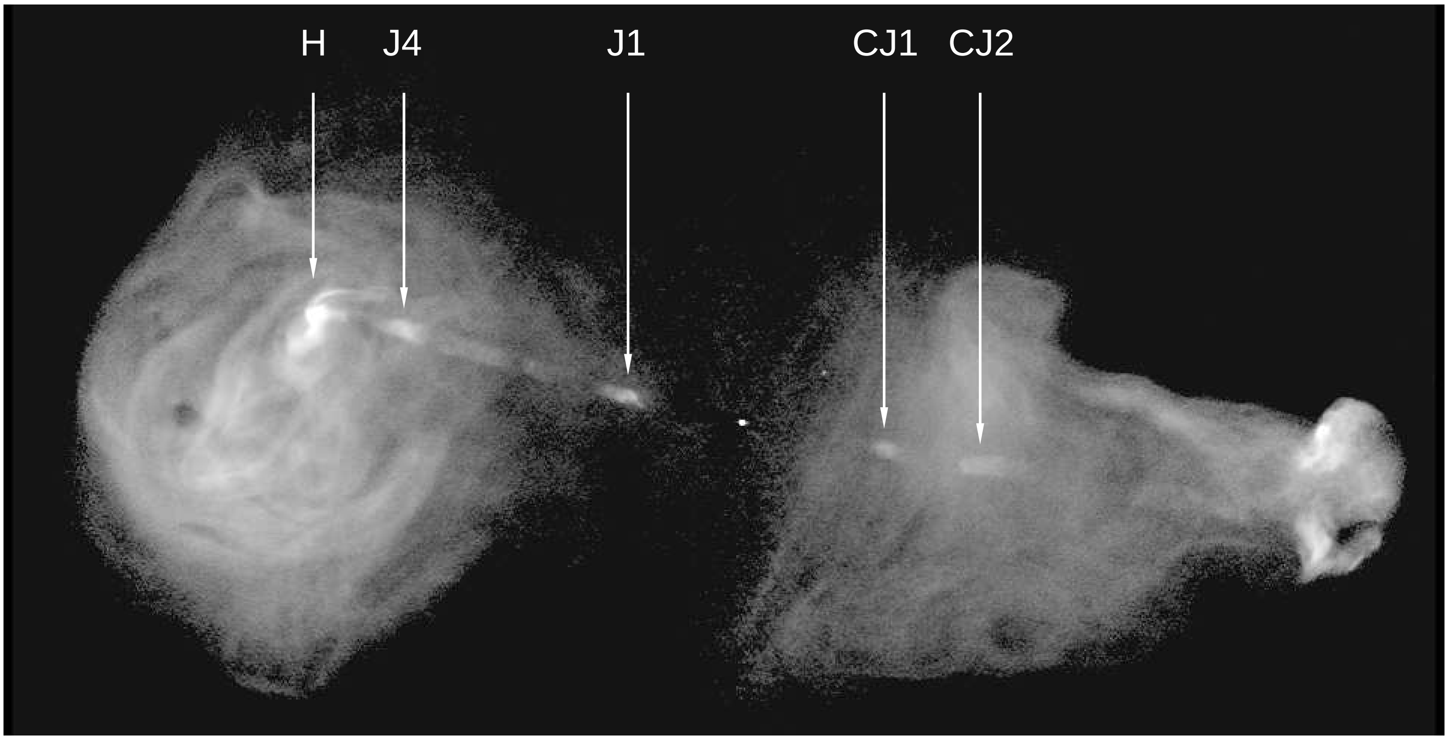

Fig. 1.— (Plate L1). Gray scale rendition of the 8.4 GHz total intensity image at $0\farcs44$ resolution, labeling the features noted in the text.

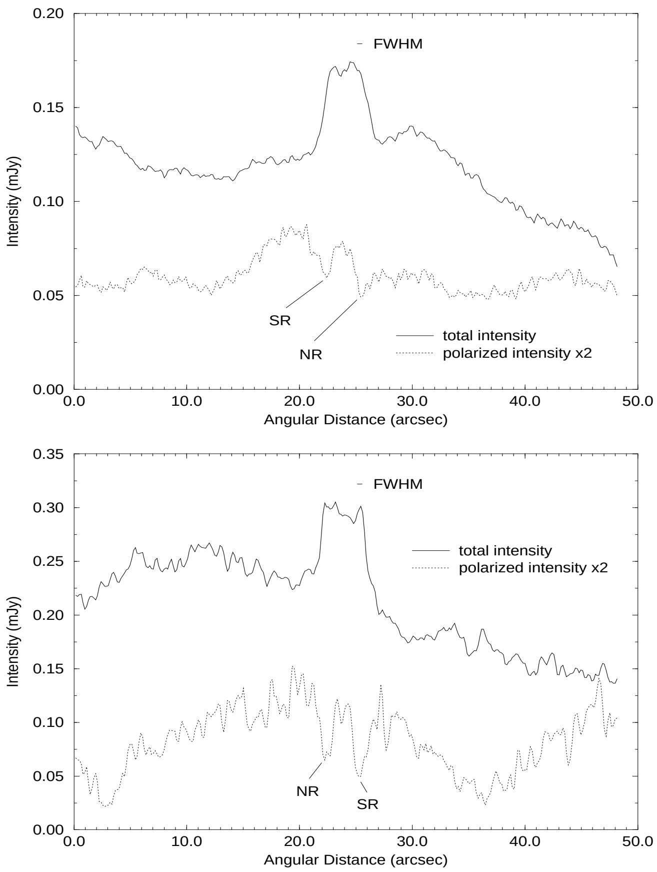

Fig. 2.— Transverse profiles of the total intensity I (solid line) and polarized intensity P (dotted line) of the jets in 3C 353 at 8.4 GHz with $0\farcs44$ FWHM resolution, averaged along the jet (upper panel) in the region between J1 and J4 and in the counterjet (lower panel) in CJ2. NR and SR mark the positions of the north and south polarization minima ("rails") associated with the jets.

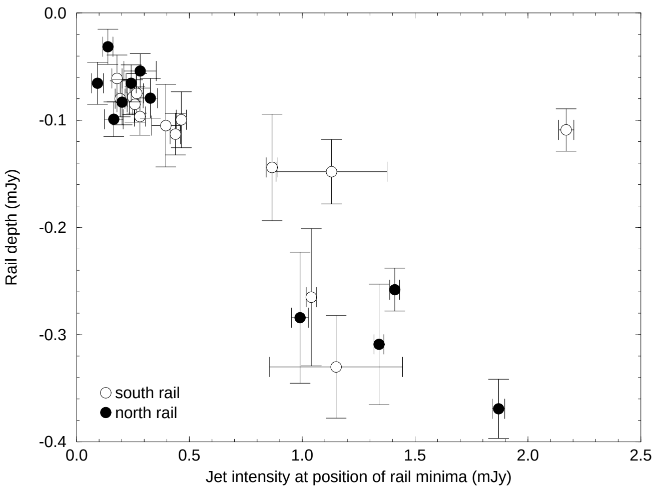

Fig. 3.— The correlation between rail depth and jet intensity measured at the rail minima at 8.4 GHz with 1.″3 FWHM resolution wherever the rail depth exceeds 3σ.

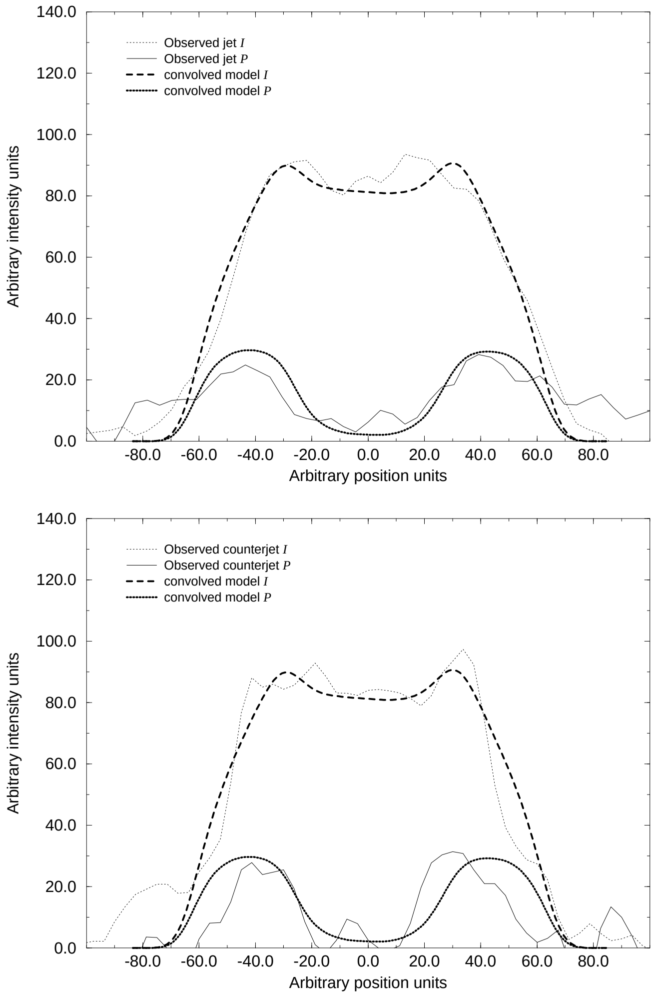

Fig. 4.— Predicted transverse I and P profiles of the model with zero emissivity in the spine, whose boundary is here at $r = 26$ (0.43 that of the jet), compared with the observed profiles. The model profiles have been convolved to the same $0\farcs44$ FWHM resolution as the observations of the jet (upper panel) and counterjet (lower panel).